

Hierarchical Segmentation of Range Images With Contour Constraints

Pierre Boulanger

University of Alberta

pierreb@cs.ualberta.ca

Gustavo Osorio

National University of Colombia

aosorio@nevado.manizales.unal.edu.co

Flavio Prieto

National University of Colombia

fprieto@nevado.manizales.unal.edu.co

Abstract

This paper describes a new algorithm to segment in continuous parametric regions range images. The algorithm starts with an initial partition of small first order regions using a robust fitting algorithm constrained by the detection of depth and orientation discontinuities. The algorithm then optimally group these regions into larger and larger regions using parametric functions until an approximation limit is reached. The algorithm uses Bayesian decision theory to determine the local optimal grouping and the complexity of the parametric model used to represent the range signal. After the segmentation process an exact description of the boundary of each region is computed from the mutual intersections of the extracted surfaces. Experimental results show significant improvement of region boundary localization. A systematic comparison of our algorithm to the most well known algorithm in the literature is presented to highlight the contributions of this paper.

1. Introduction

Tasks such as object recognition, reverse engineering, industrial inspection, or robotics, require to be able to identify real world objects from sensors capable of digitizing in 3D an environment or an object. For most of these applications an intermediate segmentation process is required to partition the data into real 3D models that can then be used for manufacturing or spatial reasoning.

One of the fundamental requirement for a good segmentation algorithm is that an accurate segmentation process must represent simultaneously large geometric shapes without the loss of edge locations. In addition to this simple criteria the following constraints on 3D segmentation algorithm must also be satisfied:

- The information produced must be accessible to high level processing;

- The process must be numerically stable and repeatable;
- One must always be able to assess the reliability of the approximation;
- The program must be able to represent the best description of the data set at the desired tolerance;
- The segmentation must be robust to signal discontinuities;
- Complex geometric models must be statistically justified.

Automatically processing range images to segment objects into CAD compatible models is a very difficult task. Currently in industry, a tedious process of manual segmentation is required to extract a correct B-rep model from the range data. Software such as CATIA V5 R13 [3] provide tools to help designers capture from 3D data a model that is compatible with the normal flow of virtual manufacturing process. The reason that most algorithms have difficulties with the segmentation process is that they rely on various feature extraction algorithms that are easily corrupted by noise and other sensor errors.

The scientific literature reports many segmentation algorithms. As classified by Hoover et al. [4] algorithms for range image segmentation falls into two basic categories, i.e., 1) region-based or 2) edge-based. There are also the so called hybrid techniques that use both region and edge information to guide the segmentation process. In many ways the proposed segmentation algorithm fall into this category. In Hoover et al. ground braking work, four of the state-of-the-art range image segmentation algorithms were analyzed systematically relative to a ground truth segmented by an expert. One of the major conclusion of this analysis is that range image segmentation is still not really a solved problem even for simple scenes containing only polyhedral objects. Later Jiang et al. [5] and Min et al. [7] confirmed

those results by further refining this comparison technique. The main problem is that in most algorithms, it is hard to detect accurately at the same time geometric surfaces and exact edge locations. This is key for the reverse engineering problem since most CAD modelling tools require an exact B-rep representation. Hoover et al. segmentation comparison framework is widely used for evaluating segmentation algorithms, including segmentation algorithms [8] for curved surface and in [7] to compute optimal segmentation parameters.

In this paper, we will analyze a new segmentation algorithm based on a hierarchical grouping of an initial partition based on a Bayesian criteria. The algorithm starts with an initial partition of the range data constrained by the detection of depth and orientation discontinuities. These constraints are then used for the seed region estimation process where a robust random sampling algorithm is used to estimate the dominant mode in the seed regions. This is an essential process to avoid contamination of the seed regions by shot noise or/and undetected discontinuities.

From this initial partition, the algorithm starts grouping these regions into larger and larger regions until the approximation error in one of the region is greater than a predetermined threshold. The algorithm then try to transform these primitives into more complex ones by using higher order parametric models. The key idea behind the algorithm is that one should start with the simplest hypothesis about the model of the data, and gradually increase the complexity of the hypothesized model as statistical evidence grows. This hierarchical region growing algorithm produce accurate estimated of each region but like in most algorithms usually at the expense of boundary localization especially with noisy data.

In order to solve this problem an intersection algorithm between adjacent surfaces was developed to re-estimate more accurately the boundary location from the segmented surfaces. It is based on a parametric intersection algorithm and can be used for planar as well as for more complex curve surfaces. Closure and smoothness of the contours is guaranteed using a snake like algorithm based on a vector flow field.

This paper present a consistent view of the grouping criterion, the generalization process based on Bayesian decision framework, and the redetermination of the region boundaries. The end result of this segmentation process is a compact representation of a scene composed of continuous surface patches usually represented as a Boundary Representation (B-rep) saved in STEP or IGES formats that can be directly loaded in advanced CAD system such as CATIA.

2. Problem Definition

In this approach to segmentation, the relevant structure of a range image is viewed as a piecewise smooth parametric polynomial contaminated by noise. A piecewise smooth parametric surface $\vec{\eta}(u, v)$ can be partitioned into N smooth surface models $\vec{f}_i(u, v; \mathbf{A}_i)$ over a connected support region Ω_i :

$$\vec{\eta}(u, v) = \sum_{i=1}^N \vec{f}_i(u, v; \mathbf{A}_i) \xi(u, v, \Omega_i) \quad (1)$$

where $\xi(u, v, \Omega_i)$ is the characteristic function of the region Ω_i , and is equal to one if $(u, v) \in \Omega_i$ and zero otherwise. The array \mathbf{A}_i is the model parameters. The function $\vec{\eta}(u, v) = (x, y, z)^T$ is a three dimensional signal corresponding to the x, y, z components.

The segmentation problem can be stated as following: given a discrete range image $\vec{r}(u_i, v_i) = (x_i, y_i, z_i)^T$ and an approximation thresholds ε_t find the N image regions Ω_i approximated by N statistically reliable functions $\vec{f}_i(u_i, v_i; \mathbf{A}_i)$ subject to:

$$\chi^2 = \frac{1}{n_l} \sum_{(u_i, v_i) \in \Omega_i} (\vec{f}_i - \vec{r})^T \Sigma^{-1} (\vec{f}_i - \vec{r}) < \varepsilon_t \quad (2)$$

The parameter n_l is equal to the number of pixels in the region Ω_i . The matrices Σ is the covariance matrices of the noise associated to the range signal and can be modelled using a technique described in [9].

The basic steps of the algorithm are the following:

1. Do an initial partitioning of the data set based on a first order parametric model using a robust fitting technique constrained by depth and orientation discontinuities.
2. Group adjacent first order regions with other first order regions or points to produce a larger first order region. Validate the grouping corresponding to the one which is the most similar based on a Bayesian criterion.
3. Loop until the similarity criterion is smaller than a predetermined threshold.
4. Generalize the first order regions to second order one if the decision is supported by statistical significance test.
5. Group adjacent first or second order regions to other points, first, or second order regions to produce a larger region corresponding to the highest order of the two. Validate the grouping corresponding to the one which is the most similar.
6. Generalize second order regions into higher order parametric polynomials using geometrical heuristics if it is supported by Bayesian decision.

7. Proceed with more grouping until no more regions are generalized.
8. Re-compute accurate boundary regions by performing surface to surface re-intersections and vector flow smoothing to guaranty closure and smoothness.

3. Signal Representation

The type of model used to represent the shape of the range data is highly constrained by the feasibility of the corresponding segmentation algorithm. A parametric Bézier polynomial is used to represent the range signal and is defined as:

$$\vec{f}_l(u, v; \mathbf{A}_l) = \sum_{i=0}^k \sum_{j=0}^k \vec{a}_{ij} B_i(u) B_j(v) \quad (3)$$

$B_m(t)$ is a Bernstein polynomial defined as:

$$B_m(t) = \frac{k!}{(k-m)!m!} t^m (1-t)^{k-m}. \quad (4)$$

This equation can be represented in matrix form by:

$$\vec{f}_l(u, v; \mathbf{A}_l) = \mathbf{A}_l \mathbf{M}_{l|uv} \quad (5)$$

where the array $\mathbf{A}_l = [\vec{a}_{00}, \vec{a}_{10}, \vec{a}_{01}, \dots, \vec{a}_{kk}]$ is the coefficients array of size $3 \times (k+1)^2$ and

$$\mathbf{M}_{l|uv} = [B_0(u)B_0(v), B_1(u)B_0(v), B_0(u)B_1(v), \dots, B_k(u)B_k(v)]^T \quad (6)$$

is the basis function matrix of size $(k+1)^2 \times 1$.

If one assume that the range data $\vec{r}(u_i, v_i)$ is corrupted by Gaussian noise of means $\vec{\mu}_r = \vec{\mu}_c = 0$ and for which the covariance matrices are equal to Σ , then the optimal model coefficients are the ones which minimize the log-likelihood function of the observations corresponding to the minimum of the standard least squared metric L^2 given by equation (2).

The minimum occurs when $\nabla_{\mathbf{A}_l} \chi^2 = 0$ which correspond in matrix form to:

$$\mathbf{T}_l = \mathbf{A}_l \mathbf{L}_l \quad (7)$$

where $\mathbf{L}_l = [\mathbf{M}_{l|u_1 v_1}, \dots, \mathbf{M}_{l|u_{n_l} v_{n_l}}]$ is a matrix of size $(k+1)^2 \times n_l$ and $\mathbf{T}_l = [\vec{r}(u_1, v_1), \dots, \vec{r}(u_{n_l}, v_{n_l})]$ a matrix of size $3 \times n_l$ corresponding to the sensor measurements. The solution correspond to the normal equation equal to:

$$\mathbf{A}_l = \mathbf{T}_l \mathbf{L}_l^T (\mathbf{L}_l \mathbf{L}_l^T)^{-1} = \mathbf{V}_l \mathbf{R}_l^{-1} \quad (8)$$

where \mathbf{R}_l is an Hermitian matrix of size $(k+1)^2 \times (k+1)^2$ corresponding to the covariance matrix of the basis functions and \mathbf{V}_l is a matrix corresponding to the correlation

between the basis functions and the measurements. Using this notation the covariance matrix of the approximation error is equal to:

$$\hat{\Sigma}_l = \mathbf{T}_l \mathbf{T}_l^T - 2\mathbf{A}_l \mathbf{V}_l^T + \mathbf{A}_l \mathbf{R}_l \mathbf{A}_l^T \quad (9)$$

The average error on the model parameters $\delta \mathbf{A}_l$ is proportional to the diagonal element of the inverse of the matrix \mathbf{R}_l , i.e.,

$$\delta \mathbf{A}_l = \frac{\mathbf{D}_l^T \mathbf{U}_l}{n_l - (k-1)^2} = [\delta \mathbf{A}_{l|i}, \delta \mathbf{A}_{l|j}, \delta \mathbf{A}_{l|k}]^T \quad (10)$$

where $\mathbf{D}_l = [\text{Diag } \hat{\Sigma}_l] = [\hat{\sigma}_{l|i}^2, \hat{\sigma}_{l|j}^2, \hat{\sigma}_{l|k}^2]$ is a 1×3 matrix corresponding to the variance of the fitting error in each orthogonal directions and is equal to the diagonal elements of the matrix $\hat{\Sigma}_l$. The matrix $\mathbf{U}_l = [\text{Diag } \mathbf{R}_l^{-1}]$ is a $1 \times (k+1)^2$ matrix where each element is the diagonal element of the covariance matrix \mathbf{R}_l^{-1}

4. Initial Partition Method

Like many region growing techniques, one needs to make an initial guess of the primitives and then iteratively refine the solution. Besl [1] used the topographic map based on the sign of Gaussian and mean curvatures to determine seed points where his algorithm grows regions of increasing size and complexity from. There is a relationship between the quality of the initial guess and the number of iterations required to converge to the final region size. Because of the importance of the initial partition, the algorithm use a robust fitting technique constrained by previously detected depth and orientation discontinuities using a morphological technique described in [2]. The algorithm uses a Least Median Square (LMS) fitting method first described by Rousseeuw and Leroy [10] which allows a robustness up to 50% outliers. The algorithm to find the initial partition is the following:

- Set the window size $L = L_{\max}$ to the maximum window size (typically 11×11).
- Find a square neighborhood of size $L \times L$ where there is no depth nor orientation discontinuities present.
- Do least median square fitting and detect the outliers (not sensitive to 50% of outliers).
- Eliminate the outlier from the window by releasing their availability to be used by other regions.
- Compute the least square model without the outliers.
- Proceed for the whole image with the same window size.

- Do the same operation with a reduced window size $L = L - 2$ until the minimum window size L_{\min} has been reached (typically 3×3).

This new initial partition technique is not sensitive to impulse noise (up to 50% of outliers) and is capable of producing excellent seed regions even for a large neighborhood.

5. Compatibility Function

A similarity function is a predicate that determine if two regions can be merged into one. Let Ω_i be a region composed of n_i points defined by the maximum likelihood model parameters $\mathbf{A}_i = (\vec{b}_{00}, \vec{b}_{10}, \dots, \vec{b}_{kk})^T$ for the range signal. Each region is also characterized by their covariance matrices $\hat{\Sigma}_i$. Let $\delta\mathbf{A}_i = (\delta\vec{b}_{00}, \delta\vec{b}_{10}, \dots, \delta\vec{b}_{kk})^T$ be the margin of error on the model parameters estimated by equation (10). Let $\{\Omega_m\}$ be the set of N_t regions adjacent to the region Ω_i and defined by the models \mathbf{A}_m with a margin of error equal to $\delta\mathbf{A}_m$. The best grouping of region Ω_i with one of its neighbors correspond to the one for which:

$$P(\Omega_b \wedge \Omega_i | \Omega_i) = \max_b \frac{\prod_{u,v \in \Omega_i} p_t(u, v | \mathbf{A}_b) p(\delta\mathbf{A}_b)}{\sum_{j=1}^{N_t} \prod_{u,v \in \Omega_i} p_t(u, v | \mathbf{A}_j) p(\delta\mathbf{A}_j)} \quad (11)$$

where $p_t(u, v | \mathbf{A}_b)$ is equal to the probability that a point in region Ω_i with coordinate u and v would be predicted by one of the model \mathbf{A}_b adjacent to Ω_i . The likelihood of grouping the region Ω_i with Ω_b is given by:

$$P(\Omega_i | \mathbf{A}_b) = \alpha \exp\left(-\frac{\hat{\sigma}_{ib}^2}{2}\right) = \prod_{u,v \in \Omega_i} p_t(u, v | \mathbf{A}_b) \quad (12)$$

where

$$\hat{\sigma}_{ib}^2 = \text{Tr}[(\mathbf{T}_i \mathbf{T}_i^T - 2\mathbf{A}_b \mathbf{V}_i^T + \mathbf{A}_b \mathbf{R}_i \mathbf{A}_b^T) \Sigma^{-1}] \quad (13)$$

is the sum of the square difference between the functions representing region Ω_b extrapolated to predict region Ω_i . The function $p(\delta\mathbf{A}_b)$ is the *a priori* probability of the region Ω_b and can be evaluated by the following equation:

$$p(\delta\mathbf{A}_b) = \omega_1 \exp\left[-\frac{1}{2}[\delta\mathbf{A}_{b|x} \Sigma_A^{-1} \delta\mathbf{A}_{b|x}^T + \delta\mathbf{A}_{b|y} \Sigma_A^{-1} \delta\mathbf{A}_{b|y}^T + \delta\mathbf{A}_{b|z} \Sigma_A^{-1} \delta\mathbf{A}_{b|z}^T]\right] \quad (14)$$

where Σ_A is equal to the true covariance matrix of the parameters \mathbf{A}_b and represents the strength of the belief that the coefficients of the matrices \mathbf{A}_b are the true value of the coefficients. In practice, the covariance matrix cannot be evaluated, but in our implementation, we artificially set the diagonal elements of the matrix Σ_A equal to β^2 and the off-diagonal to zero.

From equations (11), (12), and (13) the *a posteriori* probability of a grouping correspond to the one which maximize the numerator. If one computes the log of the numerator of equation (11), one can obtain a grouping coefficient equal to:

$$c_{ib} = \hat{\sigma}_{ib}^2 + \frac{(\hat{\sigma}_{b|x}^2 + \hat{\sigma}_{b|y}^2 + \hat{\sigma}_{b|z}^2) \text{Tr} \mathbf{R}_b^{-1}}{\beta^2(n_b - (k-1)^2)} \quad (15)$$

Using this compatibility coefficient, one can select the best groupings, by selecting from all the possible grouping the one corresponding to the minimum value.

6. Geometrical Generalization

The problem of segmentation is to find the most reliable minimal description of an image. This statement implies that the complexity of the model used by the segmentation algorithm must only be increased if there is a strong statistical evidence. Let $\hat{\sigma}_t^2$ be the approximation error of the model with the larger number of parameters $p_{\max} = (k+1)^2$ as computed by equation (9). Its value is kept as a comparison basis. In order to validate a parameter in the coefficient matrix \mathbf{A}_i the algorithm first eliminate this element from the coefficient matrix by setting it equal to zero and then compute the new approximation error $\hat{\sigma}_n^2$. The variation of the relative error is given by:

$$\frac{\hat{\sigma}_n^2 - \hat{\sigma}_t^2}{\hat{\sigma}_t^2} = \frac{\hat{\sigma}_n^2}{\hat{\sigma}_t^2} - 1 = r - 1. \quad (16)$$

The variables $\hat{\sigma}_n$ and $\hat{\sigma}_t$ are equal to the sum of the squared error for the reduced model and the full model respectively.

If the statistics r is close to unity, one may conclude with confidence that the i^{th} component of one of coefficient matrices is not statistically significant. The statistical distribution of the variable r is distributed as a Snedecor's F distribution with $\nu_1 = 1$ and $\nu_2 = n_i - p_{\max}$ degrees of freedom. The decision to reject the parameter i from the coefficient matrix with a degree of confidence α is given by:

$$P_F(r \geq r_o) = \int_{r_o}^{\infty} p_F(r) dr \geq \alpha. \quad (17)$$

In the algorithm the parameter α is set equal to 0,1.

7. Intersection of Surfaces

Once the region growing process is finished it is essential to re-adjust the boundaries of each region by performing a geometric intersection. Lets define the parametric patch for one parametric linear surface to be:

$$\begin{bmatrix} a_{11} & a_{12} & a_{13} \\ a_{21} & a_{22} & a_{23} \\ a_{31} & a_{32} & a_{33} \end{bmatrix} \begin{bmatrix} 1 \\ u \\ v \end{bmatrix} + \begin{bmatrix} C_x \\ C_y \\ C_z \end{bmatrix} = \begin{bmatrix} x \\ y \\ z \end{bmatrix} \quad (18)$$

By combining the origin term to equation (18) one can express this equation in matrix form by:

$$\mathbf{A}_i = \begin{bmatrix} a_{11} + C_x & a_{12} & a_{13} \\ a_{21} + C_y & a_{22} & a_{23} \\ a_{31} + C_z & a_{32} & a_{33} \end{bmatrix} \quad (19)$$

$$\vec{p}_i = \begin{bmatrix} 1 \\ u \\ v \end{bmatrix}; \vec{s}_i = \begin{bmatrix} x \\ y \\ z \end{bmatrix} \quad (20)$$

where $\mathbf{A}_i \cdot \vec{p}_i = \vec{s}_i$. Let $\vec{o}_i = [C_{xi}, C_{yi}, C_{zi}]^T$ be the origin vector of the plane. The equation of a vector \vec{v} at the boundary is defined by:

$$(\vec{o}_i + \vec{v}) \cdot \vec{n}_i = \vec{0} \quad (21)$$

where \vec{n} is the normal of the plane. The vector \vec{v} is determined from two adjacent plane by:

$$\vec{v} = t\vec{v}_{ij} + \vec{o}_{ij} \quad (22)$$

where \vec{o}_{ij} is a point that belong to both surface i and j and $\vec{v}_{ij} = \vec{n}_i \times \vec{n}_j$ is equal to the cross product between the two surface normals \vec{n}_i and \vec{n}_j .

One can see in Figure 1a the result of the segmentation with an overlay of the detected intersection lines and in Figure 1b the new surface edges replaced by the line equation. In some cases the new boundaries may not join the other boundaries creating gaps in the contour of the region. In order to solve this problem we used an active contour algorithm using a gradient vector flow (GVF) fields. The minimization of the active contours is achieved by solving a pair of decoupled linear partial differential equations which diffuses the gradient vectors of the binary edge map computed from the surface re-intersections. An exact description of the algorithm can be found in Xu and Prince [12]. One advantage of this algorithm over a traditional snake is that it is insensitivity to initialization and have the ability to move into concave boundary regions effectively closing a region. One can see in Figure 1c the gradient vector field for the edges illustrated in Figure 1b and in Figure 1d the resulting segmentation created by this algorithm. Using this technique, we were able to close all edges in each region creating a smooth and air tight contours, an essential condition for B-rep.

8. Results

The main purpose of this section is to evaluate the segmentation algorithm developed in this paper relative to the current state-of-the-art.

In order to make this evaluation, it is important to use a frame work that allows the comparative analysis with different techniques reported in the literature. In Hoover et

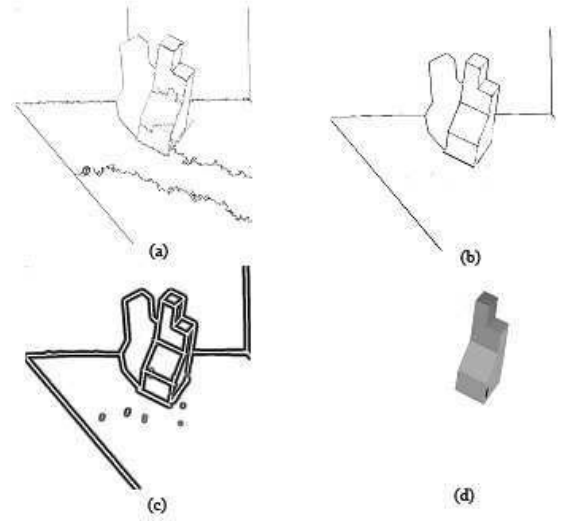


Figure 1. Segmentation with boundary correction (a) Initial segmentation with new edge candidates for boundary replacement, (b) new boundaries using line equations, (c) vector flow field computed from edge map of Figure 1b, (d) resulting segmentation after edge correction.

al. [4] the performance metric is based on a comparison of the result from automatic segmentation algorithms (Machine Segmentation - MS) with a hand made segmentation performed by an expert (Ground Truth - GT). Following this comparison process, every regions in the MS image are classified as one instance of the following five possible categories: correct detection, over-segmentation, under-segmentation, missed and noise. The evaluation process of our segmentation algorithm should take into account the fact that the optimal criteria is a function of the error obtained between the parametric model and the range data, this mean that the GT images are not involved in the fitting and clustering process. Another aspect that should be considered is that the techniques with the best performance include global information in the segmentation process, or they include additional fitting for borders calculation. Figure 2a presents the segmentation results with the segmentation algorithm developed at the University of Bern (UB) [6] which was considered the best algorithm at the time according to Hoover et al. [4] and more recently in Min et al. [7]. Figure 2b illustrate the segmentation results of our algorithm. One can notice that because of the noise one of the orientation discontinuities was miss classified. This is mainly due to the fact that during the initial partition process the local signal created by the orientation discontinu-

ities is in the same order of magnitude as the noise, hence contaminating the seed regions close to the orientation discontinuities. One can see in Figure 2c, the results of the re-intersection process and in Figure 2d the segmented object extracted automatically from its background. One can see that the re-intersection process solves the problem associated to the region growing algorithm and create a quasi perfect segmentation. As suggested by Hoover et al., we also used multiple (30) range images from USF [11] perceptron range image database to compare the results of our segmentation algorithm with the University of Bern. One can see the comparison results in Figure 3. Initially our algorithm without boundary constraints was inferior to the UB algorithm. Although if we segment the background, we had in appearance a better performance. This is due to the fact that the comparison methodology do not take into account the weight of the background pixels. On the other hand adding the boundary constraints did improve significantly our algorithm where in fact there is no major differences between ours and the UB algorithm. The main difference is that our algorithm can generalize to higher order surfaces and that the UB algorithm is limited to planar surfaces.

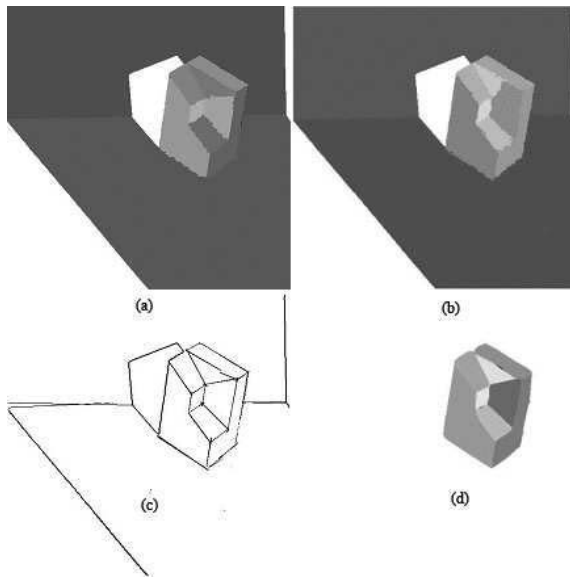


Figure 2. Segmentation results:(a) Segmentation with UB algorithm , (b) segmentation with our algorithm, (c) corrected contours, (d) new segmentation with corrected contours.

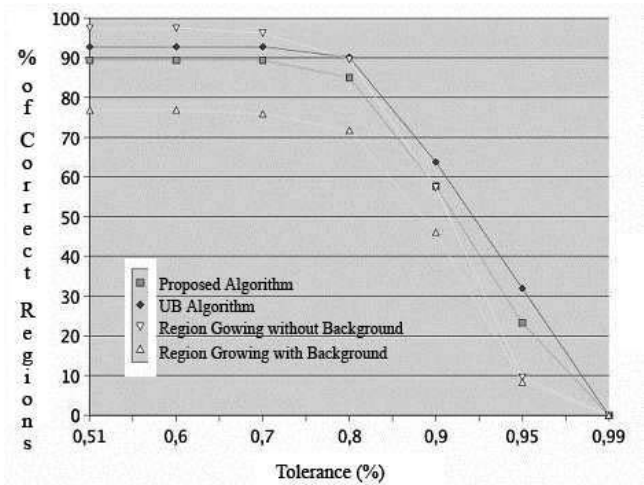


Figure 3. Comparison between the UB algorithm and the proposed algorithm.

9. Conclusion

We present, in this paper, a new hierarchical segmentation algorithm based on an optimal Bayesian grouping criterion and a re-intersection algorithm between the surfaces. In general, region growing algorithms extract information from the local to the global levels where eventually global levels get corrupted by misclassifications producing over segmentation of local information. Most algorithms do not take into account that one can use global information to correct these mistakes. This algorithm is trying to solve this problem by using surface to surface re-intersection of parametric surface patches. We have demonstrated that for planar patches this algorithm operate as well as the University of Bern algorithm with similar optimal operating conditions and without the constraints of working exclusively for planer patches. This re-intersection algorithm is a significant improvement of our previous algorithm presented in [2]. Currently our algorithm works only for first order Bézier surfaces but we are currently working on a more general surface to surface intersector that will be able to deal with surfaces with higher order polynomials. In the proposed algorithm, we have also shown that closure and smoothing of the surface contours can be easily achieved using a snake algorithm based on gradient vector flow. In the current implementation the contours of each surface patches is post-processed where each contour is approximated by B-Spline curves and the resulting model saved as a B-rep, ready to be used in a CAD system. We are also modifying our current algorithm to work on triangular meshes, a must if one want to work with multi-view data.

Acknowledgements

The authors would like to thank the National University of Colombia as well as to the University of Alberta for their institutional support in the development of this work. We would also like to thanks NSERC for their financial support.

References

- [1] P.J. Besl and R.C. Jain, *Segmentation through variable-order surface fitting*, IEEE Trans. on Pattern Analysis and Machine Intelligence, Vol. PAMI-10, no. 2, pp. 167– 192, 1988.
- [2] P.Boulanger. Extraction Multiéchelle d'éléments géométriques. Ph.D. Dissertation, Departement of Electrical and Computer Engineering, Ecole Polytechnique, University of Montreal, 1994.
- [3] Catia V5 R13 <http://www.catia.com>
- [4] A. Hoover; G. Jean-Baptiste; X. Jiang; P.J. Flynn; H. Bunke; D.B. Goldgof; K. Bowyer; D.W. Eggert; A. Fitzgibbon; R.B. Fisher, An experimental comparison of range image segmentation algorithms, IEEE Transactions on PAMI, 18(7), pp. 673-689,1996.
- [5] X. Jiang, K. Bowyer, Y. Morioka, S. Hiura, K. Sato, S. Inokuchi, M. Bock, C. Guerra, R.E. Locke, J.M.H. du Buf . Further Results of Experimental Comparison of Range Image Segmentation Algorithms. In 16 International Conference on Pattern Recognition, September 2000.
- [6] X. Jiang and H. Bunke, Fast segmentation of range images by scan line grouping, Machine Vision Application, vol. 7, no. 2, pp. 115122, 1994.
- [7] J. Min, M. Powell, and K. W. Bowyer, Automated Performance Evaluation of Range Image Segmentation Algorithms, IEEE Transactions on Systems, Man, and Cybernetics PART B: CYBERNETICS, VOL. 34, NO. 1, pp. 263-271, February 2004.
- [8] M. W. Powell, Comparing curved-surface range image segmenters, Proc. of the 6th ICCV, Bobmbay, India, pp. 286-291, 1998.
- [9] F. Prieto, T. Redarce, P. Boulanger, and R. Lepage R., *Tolerance Control with high quality 3D data*, Third Conference on 3D Digital Imaging and Modeling, Quebec, Canada, May 28th-June 1st,2001.
- [10] P.J. Rousseeuw and A.M. Leroy, *Robust regression and outlier detection*, J. Wiley and Sons,1987.
- [11] University of Southern Florida Range Image Database, <http://marathon.csee.usf.edu/range/DataBase.html>
- [12] Ch. Xu, J. L. Prince. Gradien Vector Flow: A New External Force for Snakes. In IEEE Proceedings on Computer Vision and Pattern Recognition, 1997.